PRAMANA
— journal of
physics

Vol. 59, No. 2
August 2002
pp. 243–254

Developments in quantum information processing by nuclear magnetic resonance: Use of quadrupolar and dipolar couplings

ANIL KUMAR[a,b,*] K V RAMANATHAN[b], T S MAHESH[a], NEERAJ SINHA[a] and K V R M MURALI[a,c]

[a]Department of Physics; [b]Sophisticated Instruments Facility, Indian Institute of Science, Bangalore 560 012, India

[c]Present address: Media Lab, M.I.T., Cambridge, USA

[*]Author to whom correspondence should be addressed. Email: anilnmr@physics.iisc.ernet.in

Abstract. Use of dipolar and quadrupolar couplings for quantum information processing (QIP) by nuclear magnetic resonance (NMR) is described. In these cases, instead of the individual spins being qubits, the 2^n energy levels of the spin-system can be treated as an n-qubit system. It is demonstrated that QIP in such systems can be carried out using transition-selective pulses, in CH_3CN, $^{13}CH_3CN$, ^{7}Li ($I = 3/2$) and ^{133}Cs ($I = 7/2$), oriented in liquid crystals yielding 2 and 3 qubit systems. Creation of pseudopure states, implementation of logic gates and arithmetic operations (half-adder and subtractor) have been carried out in these systems using transition-selective pulses.

Keywords. Quantum information processing; qubit; nuclear magnetic resonance quantum computing.

PACS No. 03.67.-a

1. Introduction

Ever since the suggestion by Feynman in 1982 that quantum mechanical devices should simulate quantum systems much more efficiently than classical computers [1], the search for quantum algorithms has gained great impetus. Several algorithms have been developed [2–4] which validate the premise of Feynman. Shor's prime factorization algorithm [4] is creating panic among cryptographers [5]. Grover's search algorithm has given new dimension for data base search [3]. Quantum Fourier transform [6], quantum error correction [7,8], quantum teleportation [9], quantum logic gates [6–8], quantum simulation [1,10–15], quantum cloning [16] and Deutsch–Jozsa algorithm [2] have created a lot of excitement in scientific circles. Efforts are being made to develop further algorithms and for experimental realization of quantum computers. The experimental techniques being suggested include quantum electrodynamics, trapped ions, quantum dots and nuclear magnetic resonance (NMR) [7,8]. Of these NMR has shown the maximum progress [16–42]. Using NMR,

people have so far demonstrated preparation of pseudopure states [20–33], implementation of logic gates and Deutsch–Jozsa algorithm using both one- and two-dimensional NMR [17–19,28,34–37], creation of Einstein–Podolsky–Rosen (EPR) states [38], quantum state tomography [24,39,40], implementation of Grover's search algorithm [41] and Shor's factorization algorithm [42].

Most of the above have been implemented by NMR of spin-1/2 nuclei coupled to each other by spin–spin (J) couplings. The major requirement for a spin system to act as a device for quantum information processing is qubit addressability. This is achieved in spin-1/2 systems by the nuclei having different Larmor frequencies and finite unequal mutual couplings among all the spins. The J-coupling is mediated among nuclei through the covalent network, and becomes vanishingly small between nuclei which are more than 4 to 5 bonds away. This imposes a natural limit on the number of qubits an NMR system utilizing J-couplings can have. Here we describe the possibilities of utilizing dipolar couplings among spin-1/2 nuclei and quadrupolar couplings in spin-3/2 and spin-7/2 nuclei. These couplings are averaged to zero in rapidly and isotropically reorienting molecules in liquid state and become too large and too many in the solid state. However, for molecules partially oriented in anisotropic media such as liquid crystals, these systems give sharp spectral lines arising from reduced couplings. Such systems can then be treated as suitable candidates for quantum information processing by NMR, the aim and objective being that one can possibly increase the number of qubits in NMR quantum information processing protocol.

2. Dipolar coupled spin-1/2 nuclei

The dipolar couplings among spin-1/2 nuclei are larger in magnitude and longer in range compared to the spin–spin (J) couplings. Therefore such systems hold the promise of increasing the number of qubits in NMR. The feasibility of using dipolar coupled spin 1/2 nuclei for quantum information processing by NMR was first demonstrated by Yannoni *et al* [43]. Later, Fung demonstrated the feasibility of using CH_3CN molecule partially oriented in a liquid crystal [44], wherein the three dipolar coupled protons yield a 1:2:1 triplet in the NMR spectrum. Using this system, Fung demonstrated creation of pseudopure states and implementation of an implicit C-NOT gate. Further use of the system for computations requires that the problem of the degeneracy of transitions belonging to different symmetric states of an equivalent H_3 group is addressed. Here we describe an improved method for creation of pseudopure states and implementation of a complete set (24) of one-to-one reversible 2-qubit gates using transition-selective pulses. The Hamiltonian and the eigenstates in this case have a C_3 symmetry, dividing the eight eigenstates into three symmetry manifolds. The symmetric (A) manifold (figure 1a) has four eigenstates and there are a pair of doublet (E) manifolds. The A manifold has three transitions with the intensity ratio of 3:4:3. The transitions of the E manifold overlap with the central transition of the A manifold, yielding a 3:6:3 triplet (figure 1b). We have earlier described a method of selection of symmetric states (SOSS) and then used the four eigenstates of the symmetric manifold as a two-qubit system [45]. Similarly, we have used a ^{13}C-labeled $^{13}CH_3CN$ molecule oriented in the liquid crystal matrix. The carbon-13 (spin-1/2) has a different Larmor frequency ($\sim$1/4th of the proton) and has dipolar couplings to the protons, and this system therefore yields eight eigenstates belonging to the symmetric (A) manifold, which can then

be treated as a three qubit system [45]. We have also demonstrated SOSS for this system [45]. After implementation of SOSS in these two systems, we have created pseudo- pure states and implemented logic gates using one- and two-dimensional NMR methods [45]. Some of these results are summarized in the following subsections.

2.1 *Preparation of pseudopure states*

Certain quantum algorithms such as Shor's factorization algorithm requires that the quantum system be in a pure state before the implementation of the algorithm. When only one of the eigenstates of a system is populated the system is said to be in a pure state. This poses unrealistic experimental conditions such as zero Kelvin temperature or an infinitely high magnetic field. It has been suggested that since all NMR results depend only on differences in populations of various eigenstates, one can create population-distribution such that all levels except one have equal populations. Such a state has been termed as a 'pseudopure state' and gives results which are identical to the 'pure state' except for the low signal/noise. Using pseudopure states, one can use NMR of molecules at room temperatures in the usual laboratory magnetic fields for quantum information processing.

Figure 1c shows the NMR spectrum of the protons of CH_3CN partially oriented in a liquid crystal, after the selection of symmetric states (SOSS). This spectrum arises exclusively from the symmetric states and has the intensity ratio 3:4:3 corresponding to the equal population differences between various eigenstates of the symmetric manifold, shown schematically on the right-hand side (rhs). The equal equilibrium population differences correspond to a high-temperature (Zeeman energy $\ll kT$) and a high-field (dipolar coupling $\ll$ Zeeman energy) approximation, which are very well satisfied [46]. The central transition has higher intensity compared to outer transitions due to the higher value of the matrix elements of the observation operator $I_x^{(2,3)}$ connecting states $|2\rangle$ and $|3\rangle$. We have labeled the four eigenstates as 00, 01, 10 and 11 corresponding to a two-qubit system. Here we have adopted a labeling scheme with 00 being the lowest and 11 the highest energy state. Later in spin-7/2 case, we will show that the labeling scheme can be freely changed to suit the logic operation at hand.

Starting from such a population distribution after SOSS, various pseudopure states can be easily created using transition-selective π and $\pi/2$ pulses. A transition selective π pulse interchanges the population of selected states while a $\pi/2$ pulse (followed by a gradient/homospoil DC magnetic field pulse along the Z-direction to destroy the coherences) equalizes their populations to an average value. The $|00\rangle$ pseudopure state is created by first applying a π pulse between $|11\rangle$ and $|10\rangle$, interchanging their populations followed by a $\pi/2$ pulse between $|10\rangle$ and $|01\rangle$ (followed by the gradient pulse), yielding the population distribution corresponding to $|00\rangle$ pseudopure state, as shown on the rhs of figure 1d. A π pulse on $|01\rangle$ and $|00\rangle$ then creates the population distribution given on the rhs of figure 1e corresponding to the $|01\rangle$ pseudopure state. Other pseudopure states can be similarly created as shown in figure 1. The spectra obtained using a small angle pulse at the end of these operations reflect the new population distribution confirming the creation of the pseudopure states.

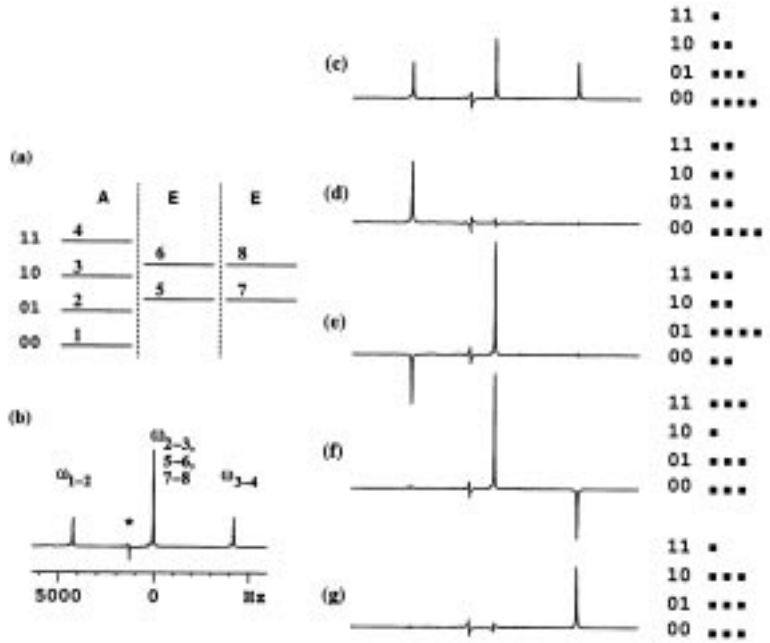

Figure 1. (**a**) Energy level diagram showing quartet (A) and doublet (E) manifolds of oriented CH_3CN system and the two-qubit labeling scheme of the A manifold, (**b**) the equilibrium ^1H spectrum, (**c**) the spectrum after SOSS, and spectra corresponding to different pseudopure states (**d**) $|00\rangle$, (**e**) $|01\rangle$, (**f**) $|10\rangle$, and (**g**) $|11\rangle$. The states and representative relative deviation populations are given on the rhs. The pseudopure states are prepared using the spatial averaging technique. The pulse sequences for preparing pseudopure states are as follows: (**d**) $\pi(10 \leftrightarrow 11) - \pi/2(01 \leftrightarrow 10)G$, (**e**) state of (**d**) followed by $\pi(00 \leftrightarrow 01)G$, (**f**) state of (**g**) followed by $\pi(11 \leftrightarrow 10)\ G$, and (**g**) $\pi(01 \leftrightarrow 10) - \pi/2(00 \leftrightarrow 01)G$.

2.2 *Logic gates*

In the two-qubit system of the symmetric states of the oriented CH_3CN molecule, various logic gates have been implemented after SOSS, using transition-selective pulses. It may be mentioned here that since a spin is not a qubit, one can not use the coupling evolution method using spin-selective pulses, as is generally the practice for weakly coupled spin-1/2 nuclei [18,19]. However, the algorithm of transition-selective pulses which we have followed in several earlier works [17,28,37] is valid and works extremely well. For example, starting from an equilibrium population distribution after SOSS (shown in figure 2a which is also labeled as NOP, No OPeration gate), a NOT1 gate (index 1 indicates NOT operation on first qubit with second qubit remaining unchanged) requires π (non-selective) $\pi(00 \leftrightarrow 01)$ $\pi(10 \leftrightarrow 11)$ (figure 2b); NOT2 requires $\pi(00 \leftrightarrow 01)$ $\pi(10 \leftrightarrow 11)$ (figure 2c); NOT on both qubits requires a non-selective π pulse (figure 2d). Figure 2 contains a complete set of reversible one-to-one 2 qubit gates. The pulse scheme for various gates are given in ref. [45].

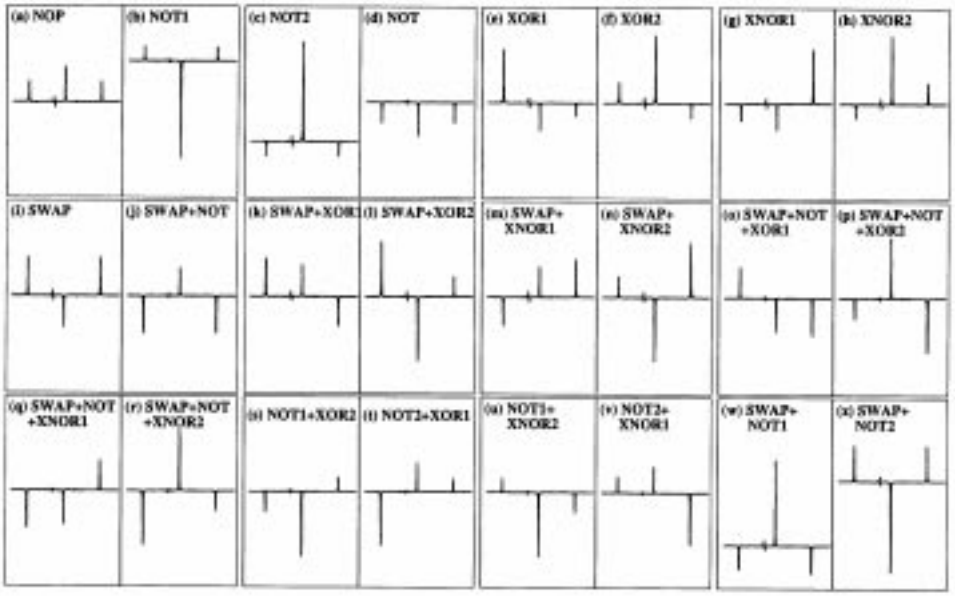

Figure 2. ^{1}H spectra of oriented CH_3CN corresponding to a complete set of 2-qubit one-to-one gates implemented (after applying SOSS) using transition-selective rf pulses. The unitary operator and pulse sequence corresponding to each gate are given in [45].

3. Use of quadrupolar ($I = 3/2$ and $I = 7/2$) nuclei

A qudrupolar nucleus of spin I has $2I + 1$ energy levels and $2I$ single quantum transitions which are equispaced if only the first-order quadrupolar interaction is operative. For molecules partially oriented in anisotropic media, such as liquid crystals, such a condition is often satisfied. If $2I + 1 = 2^n$, such a system can be treated as an n-qubit system [47,48]. One of the advantages of such systems and the dipolar coupled systems over J-coupled systems is that the coupling values are one to two orders of magnitude larger, allowing the use of correspondingly shorter transition selective pulses, with greater ease and shorter computational time. Here we demonstrate the use of a spin-3/2 (^{7}Li) and spin-7/2 (^{133}Cs) nuclei in molecules oriented in liquid crystal matrices as 2- and 3-qubit systems, respectively. We create pseudopure states, implement logic gates and half-adder and subtractor logics using transition-selective pulses. While the feasibility of using these systems as qubits have been demonstrated earlier, very little computations were performed [47,49].

3.1 *2-qubit system using ^{7}Li ($I = 3/2$)*

Figure 3b shows the three lines of ^{7}Li NMR spectrum (1.15 kHz splitting) of $LiBF_4$ oriented in a liquid crystal. This spectrum obtained at 310 K and at 194.37 MHz in a Bruker

DRX-500 NMR spectrometer results from the quadrupolar-perturbed four Zeeman energy levels of a spin-3/2 system, shown schematically in figure 3a. The equilibrium spectrum has an intensity ratio of 1:1.6:1 corresponding to equal population differences between the adjacent energy levels (under high temperature and high field approximations) which are schematically shown on the rhs of figure 3c.

Pseudopure states in this system were earlier created using double quantum pulses [47]. We have instead created pseudopure states using transition-selective single quantum pulses, which are much easier to create and implement [48]. Figures 3c–g summarize the creation of various pseudopure states. The equilibrium spectrum and the schematic representation of equilibrium population distribution are shown in figure 3c. The $|11\rangle$ pseudopure state is created by applying a $\pi(1 \leftrightarrow 2)$, which interchanges the populations of levels 1 and 2, followed by a $\pi/2(0 \leftrightarrow 1)$, which equalizes the populations of levels 0 and 1 to an average value, followed by a gradient pulse which destroys the coherences created by $\pi/2(0 \leftrightarrow 1)$. This results in the pseudopure state $|11\rangle$ (figure 3d). Similarly other pseudo- pure states have been created using transition-selective π and ($\pi/2+$ gradient) pulses as shown in figure 3.

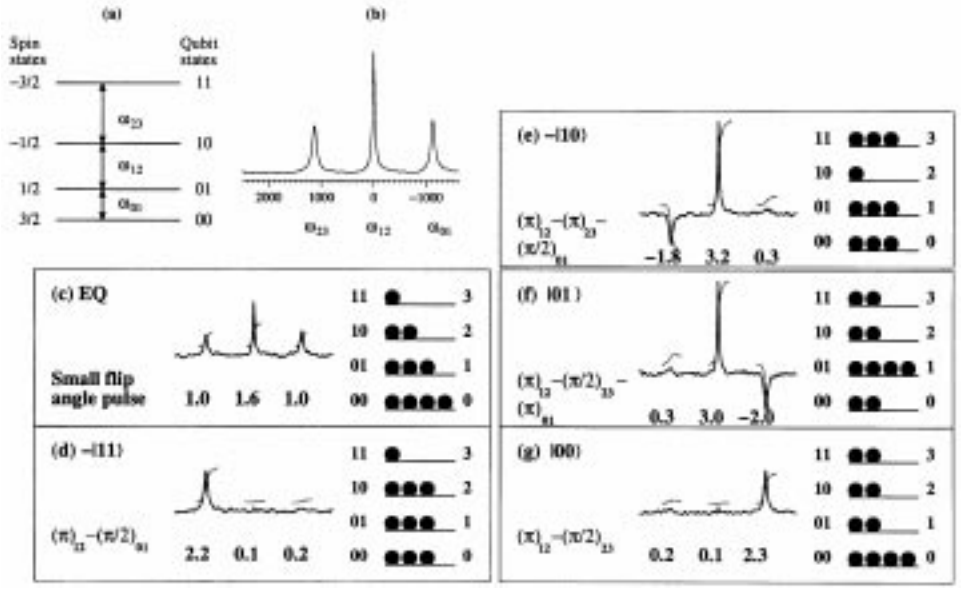

Figure 3. (**a**) Schematic energy level diagram for a spin-3/2 system and (**b**) equilibrium ^{7}Li NMR spectrum of $LiBF_4$ oriented in a liquid crystalline matrix at 310 K, obtained using a hard $\pi/2$ pulse with a Bruker DRX-500 NMR spectrometer. Equilibrium spectrum obtained using a small flip angle pulse (**c**) and spectra corresponding to different pseudo-pure states (**d–g**). All spectra are shown in the same scale. Integrated intensities of each peak are shown below each spectrum. The population distribution in each case is shown on the rhs. The pulse sequence used for creation of the pseudopure state in each case is shown on the lhs.

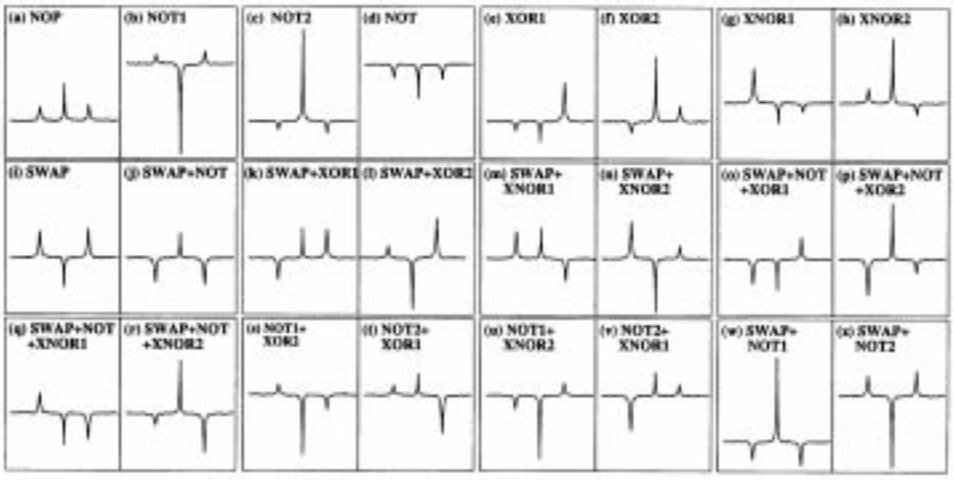

Figure 4. ^{7}Li spectra corresponding to 24 one-to-one logic gates. These gates are implemented using a non-selective inversion pulse (π) on all the transitions and a ω_{ij} transition-selective inversion pulse. The unitary operators and the pulse sequences corresponding to these gates are given in ref. [48].

Figure 4 gives a complete set of the 24 reversible one-to-one two-qubit gates implemented using transition-selective pulses. The truth table, the circuit diagram and the pulse sequence for each gate are given in ref. [48]. The spectra shown in figure 4 confirm the implemented gate operations.

3.2 *3-qubit system using* ^{133}Cs $(I = 7/2)$

The equilibrium NMR spectrum of ^{133}Cs oriented in a lyotropic liquid crystal containing a mixture of cesium pentadecaflouro octonoate and D_2O at 293 K recorded at 65.59 MHz in the DRX-500 NMR spectrometer is given in figure 5a. This seven-line equispaced (quadrupolar splitting of 9.25 kHz) spectrum results from the equal population differences of the eight energy levels. The equilibrium spectrum has theoretical intensities in the ratio of 7:12:15:16:15:12:7 due to differences in the matrix elements between the various eigenstates of this $(I = 7/2)$ spin system, matching with the integrated experimental intensities (within experimental errors). The eight eigenstates of this system can be treated as a 3-qubit system [49–51] with a conventional labeling of the states in increasing energy as $7/2 \equiv |000\rangle$, $5/2 \equiv |001\rangle$, $3/2 \equiv |010\rangle$, $1/2 \equiv |011\rangle$, $-1/2 \equiv |100\rangle$, $-3/2 \equiv |101\rangle$, $-5/2 \equiv |110\rangle$, and $-7/2 \equiv |111\rangle$. We demonstrate implementation of the half-adder (HA) and subtractor (SUB) logics using this system.

Half-adder and subtractor

Classically a half-adder (HA) operation is defined on two bits as the 'sum' = $\mathsf{A} \oplus \mathsf{B}$ and 'carry' = $\mathsf{A} \wedge \mathsf{B}$, where $\oplus$ indicates addition modulo 2 and $\wedge$ indicates the 'AND' operation.

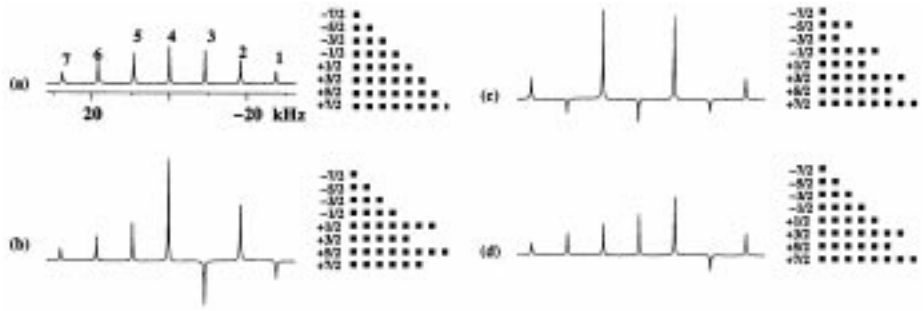

Figure 5. (**a**) The equilibrium spectrum of ^{133}Cs of the lyotropic liquid crystal consisting of mixture of cesium pentadecaflouro octanoate and D_2O at 293 K recorded at 65.59 MHz in a 11.8 T (500 MHz) NMR spectrometer. The transitions are labeled in increasing frequency, as indicated in table 3. Also shown schematically on the rhs are the equilibrium populations of various energy levels. The spectra and the populations after the implementations of (**b**) the half-adder (eq. (3)), (**c**) the subtractor (eq. (4)) and (**d**) the C^2-NOT gate (implemented by a single transition-selective π pulse on transition 2).

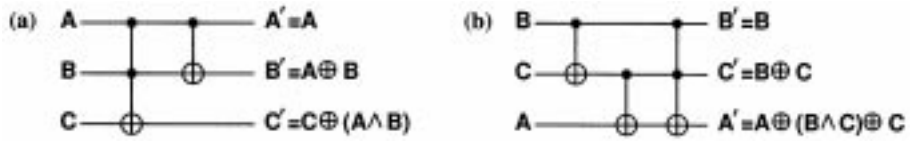

Figure 6. Circuit diagrams of (**a**) a reversible half-adder and (**b**) a reversible subtractor. In the case of the half-adder, B' is the sum and C' is the carry, and in the case of the subtractor, C' is the subtraction and A' is the borrow. .

Table 1. Truth tables of an irreversible half-adder and an irreversible subtractor.

Input		Half-output	Adder	Subtractor output	
A	B	A+B	Carry	A-B	Borrow
0	0	0	0	0	0
0	1	1	0	1	1
1	0	1	0	1	0
1	1	0	1	0	0

From the truth table of HA, given in table 1, it is noted that the input to output mapping is many-to-one and is thus irreversible. Since quantum operations are carried out using unitary operators, they have to be reversible. This reversibility can be achieved using an ancillary bit. The truth table and the circuit diagram of the HA using an ancillary bit are given in table 2 and figure 6a, respectively. In this scheme the bit C in the input and the bit A in the output are redundant.

Table 2. Input and output states of a reversible half-adder and a reversible subtractor using the conventional labeling scheme.

			Output ($A'B'C'$)	
Transition	Spin state	Input (ABC)	Half-adder	Subtractor
7{	−7/2	111	100	110
6{	−5/2	110	101	111
5{	−3/2	101	111	001
4{	−1/2	100	110	100
3{	1/2	011	011	010
2{	3/2	010	010	011
1{	5/2	001	001	101
	7/2	000	000	000

The classical subtractor operation using two bits is also irreversible (table 1) and can be made reversible using an ancillary bit (table 2 and figure 6b). Here the bit A in the input and the bit B in the output are redundant.

Table 2 contains truth tables for a 3-qubit system having eight input-outputs, of which only four are needed for both the half-adder and subtractor. The rest of four states with C=1 for HA and A=1 for subtractor and their outputs are not needed, but give complementary carry and borrow outputs. In effect using complete 3-bit truth table of table 2, one obtains the carry and borrow and their complement in half-adder and subtractor. The complement may be useful in some other arithmetic operations. The HA operation given in table 2 can be carried out using a series of transition-selective inversion (π) pulses given by the sequence

$$\text{HA} = \pi_7\pi_6\pi_5\pi_7\pi_6, \tag{1}$$

where the subscripts refer to the transition numbers given in table 2 (column 1) and figure 5a. The order of pulses read from right to left in eq. (1), such that first pulse is π_6. The output of the HA is given in column 4 of table 2.

The subtractor needs 9 transition-selective pulses in the sequence

$$\text{subtractor} = \pi_3\pi_2\pi_3\pi_5\pi_4\pi_3\pi_2\pi_5\pi_7, \tag{2}$$

yielding the output given in column 5 of table 2.

The pulse sequences (for HA and subtractor) given in eqs (1) and (2) are both optimal (minimum pulses) for the present labeling. The number of transition-selective pulses needed for the implementation of the HA and subtractor logics can be decreased if we adopt a labeling scheme of the energy levels different from the one given in table 2. The labeling scheme of table 2 labels energy levels in increasing energy. However, there is no compelling argument in favor of this labeling scheme. Any labeling scheme should be acceptable so long as each energy level is attached with one distinct label, and this label is not changed during the entire set of computations. We have found that by labeling the states which interchange under a set of operations (i.e., are connected by a single quantum transition) sequentially, we can reduce the number of pulses needed for carrying out a set of operations.

Table 3. Input and output states of a half-adder and a subtractor using an optimized labeling scheme. The circuit diagrams of the half-adder and subtractor are shown in figure 6. The output of the Toffoli (C^2-NOT) gate is $A'=A,\ B'=B,\ C'=C\oplus(A\wedge B)$.

			Output ($A'B'C'$)		
Transition	Spin state	Input (ABC)	Half-adder	Subtractor	C^2-NOT
	−7/2	000	000	000	000
7{	−5/2	010	010	011	010
6{	−3/2	011	011	010	011
5{	−1/2	001	001	101	001
4{	1/2	101	111	001	101
3{	3/2	110	101	111	111
2{	5/2	111	100	110	110
1{	7/2	100	110	100	100

For example, 111 interchanges with 110 in HA and remains unchanged in subtractor. 101 interchanges with 001 in HA and 011 with 010 in subtractor. Thus by placing 100, 111, 110, 101, 001, 011, 010 and 000 in an increasing order as shown in table 3, one can execute the HA logic by the following operator,

$$\mathrm{HA} = \pi_1\pi_3\pi_2, \tag{3}$$

and the subtractor by

$$\mathrm{subtractor} = \pi_2\pi_4\pi_6. \tag{4}$$

This leads to a minimum number of single quantum transition-selective π pulses for implementation of these logic operations. While we believe that the labeling scheme of table 3 is optimum (needs the minimum number of single quantum transition-selective π pulses) for implementation of the HA and subtractor operations, it is by no means unique. This labeling scheme has been arrived at by trial and error. However, for larger number of qubits and for a larger set of computations the search for the optimal labeling scheme will need to follow some systematic logic [51].

The experimental implementation of the HA and subtractor operations using the labeling scheme of table 3 and pulse sequences of eqs (3) and (4) are given in figures 5b and 5c, respectively. The final population differences are shown schematically on the rhs and the corresponding spectra on the lhs of figure 5. The modified populations are the results of three unitary transforms corresponding to eqs (3) and (4). The observed spectra of figure 5b qualitatively confirms the population distribution shown schematically on the rhs of figure 5b. Similarly, it can be shown that the spectra of figure 5c corresponds to the population distribution given in the rhs of figure 5c confirming the operation of the subtractor. It may be mentioned that π_3 and π_1 in the half-adder and all the pulses in the subtractor commute and can be applied simultaneously using a modulator. The HA then reduces to two non-commuting operations, and the subtractor to a single operation. Table 3 also contains the truth table for a C^2-NOT operation, and the corresponding spectrum obtained using a single transition-selective π pulse is shown in figure 5d.

4. Conclusions

This paper demonstrates that dipolar and quadrupolar coupled nuclei can be used for logical operations and eventually for quantum information processing (QIP). The hope and aim of the present work is that using such systems one can increase the number of qubits in NMR based QIP. All operations have been carried out using single quantum transition-selective radio frequency pulses.

Acknowledgements

We thank Dr. J P Bayle, Universite de Paris-Sud, Orsay, France for providing the liquid crystals used in this work. We also thank Prof. Malcolm Levitt for useful discussions. The use of DRX-500 FTNMR spectrometer of the Sophisticated Instruments Facility, Indian Institute of Science, Bangalore funded by the Department of Science and Technology, New Delhi, is also gratefully acknowledged.

References

[1] R P Feynmann, *Int. J. Theor. Phys*. **21**, 467 (1982)
[2] D Deutsch and R Jozsa, *Proc. R. Soc. London* **A439**, 553 (1992)
[3] L K Grover, *Phys. Rev. Lett.* **79**, 325 (1997)
[4] P W Shor, *SIAM J. Comput.* **26**, 1484 (1997)
[5] C H Bennett and D P DiVincenzo, *Nature* **404**, 247 (2000)
[6] J Preskill, *Lecture notes on quantum computation*, http://theory.caltech.edu/people/preskill/ph229/
[7] M A Nielsen and I L Chuang, *Quantum computation and quantum information* (Cambridge University Press, 2000)
[8] D Bouwmeester, A Ekert and A Zeilinger, *The physics of quantum information* (Springer, 2000)
[9] C H Bennett, G Brassard, C Crepeau, R Jozsa, A Peres and W K Wootters, *Phys. Rev. Lett.* **70**, 1895 (1993)
[10] S Lloyd, *Science* **273**, 1073 (1996)
[11] C Zalka, *Proc. R. Soc. London* **A454**, 313 (1998)
[12] D S Abrams and S Lloyd, *Phys. Rev. Lett.* **79**, 2586 (1997)
[13] D A Lidar and O Biham, *Phys. Rev.* **E56**, 3661 (1997)
[14] S Somaroo, C H Tseng, T F Havel, R Laflamme and D G Cory, *Phys Rev. Lett.* **82**, 5381 (1999)
[15] C H Tseng, S Somaroo, Y Sharf, E Knill, R Laflamme, T F Havel and D G Cory, *Phys. Rev.* **A61**, 012302 (1999)
[16] H K Cummins, C Jones, A Furze, N F Soffe, M Mosca, J M Peach and J A Jones, quant-ph/0111098
[17] Kavita Dorai, T S Mahesh, Arvind and Anil Kumar, *Curr. Sci.* **79**, 1447 (2000)
[18] D G Cory, R Laflamme, E Knill, L Viola, T F Havel, N Boulant, G Boutis, E Fortunato, S Lloyd, R Martinez, C Negrevergne, M Pravia, Y Sharf, G Teklemariam, Y S Weinstein and W H Zurek, quant-ph/0004104
[19] J A Jones, *Progr. Nucl. Magn. Spect.* **38**, 325 (2001)
[20] D G Cory, A F Fahmy and T F Havel, *Proc. Natl. Acad. Sci. USA* **94**, 1634 (1997)
[21] N Gershenfeld and I L Chuang, *Science* **275**, 350 (1997)
[22] E Knill, I L Chuang and R Laflamme, *Phys. Rev.* **A57**, 3348 (1998)

[23] D G Cory, M D Price and T F Havel, *Physica* **D120**, 82 (1998)
[24] I L Chuang, N Gershenfeld, M G Kubinec and D W Leung, *Proc. R. Soc. London* **A454**, 447 (1998)
[25] D G Cory, W Maas, M Price, E Knill, R Laflamme, W H Zurek, T F Havel and S S Somaroo, *Phys. Rev. Lett.* **81**, 2152 (1998)
[26] E Knill, R Laflamme, R Martinez and C H Tseng, *Nature* **396**, 52 (1998)
[27] L M K Vandersypen, C S Yannoni, M H Sherwood and I L Chuang, *Phys. Rev. Lett.* **83**, 3085 (1999)
[28] Kavita Dorai, Arvind and Anil Kumar, *Phys. Rev.* **A61**, 042306 (2000)
[29] U Sakaguchi, H Ozawa and T Fukumi, *Phys. Rev.* **A61**, 042313 (2000)
[30] Y Sharf, T F Havel and D G Cory, *Phys. Rev.* **A62**, 052314 (2000)
[31] E Knill, R Laflamme, R Martinez and C H Tseng, *Nature* **404**, 368 (2000)
[32] T S Mahesh and Anil Kumar, *Phys. Rev.* **A64**, 012307 (2001)
[33] A K Khitrin and B M Fung, *J. Chem. Phys.* **112**, 6963 (2000)
[34] J A Jones and M Mosca, *J. Chem. Phys.* **109**, 1648 (1998)
[35] N Linden, H Barjat and R Freeman, *Chem. Phys. Lett.* **296**, 61 (1998)
[36] Z L Madi, R Bruschweiler and R R Ernst, *J. Chem. Phys.* **109**, 10603 (1998)
[37] T S Mahesh, Kavita Dorai, Arvind and Anil Kumar, *J. Magn. Reson.* **148**, 95 (2001)
[38] M Marjanska, I L Chuang and M G Kubinec, *J. Chem. Phys.* **112**, 5095 (2000)
[39] Ranabir Das, T S Mahesh and Anil Kumar, *Phys. Rev. Lett.* (communicated)
[40] Ranabir Das, T S Mahesh and Anil Kumar, *J. Magn. Reson.* (communicated)
[41] I L Chuang, N Gershenfeld and M Kubinec, *Phys. Rev. Lett.* **80**, 3408 (1998)
[42] L M K Vandersypen, M Steffen, G Breyta, C S Yannoni, M H Sherwood and I L Chuang, *Nature* **414**, 883 (2001)
[43] C S Yannoni, M H Sherwood, D C Miller, I L Chuang, L M K Vandersypen and M G Kubinec, *Appl. Phys. Lett.* **75**, 3563 (1999)
[44] B M Fung, *Phys. Rev.* **A63**, 022304 (2001)
[45] T S Mahesh, Neeraj Sinha, K V Ramanathan and Anil Kumar, *Phys. Rev.* **A65**, 022312 (2002)
[46] A Abragam, *The principles of nuclear magnetism* (Oxford University Press, 1961)
[47] A K Khitrin and B M Fung, *J. Chem. Phys.* **112**, 6963 (2000)
[48] Neeraj Sinha, T S Mahesh, K V Ramanathan and Anil Kumar, *J. Chem. Phys.* **114**, 4415 (2001)
[49] A Khitrin, H Sun and B M Fung, *Phys. Rev.* **A63**, 020301(R) (2001)
[50] A K Khitrin and B M Fung, *Phys. Rev.* **A64**, 032306 (2001)
[51] K V R M Murali, Neeraj Sinha, T S Mahesh, M H Levitt, K V Ramanathan and Anil Kumar, *Phys. Rev. A* (accepted) (in press)